

# Solvent Effects on the Spectroscopic Properties of Styrylquinolinium Dyes Series

Beata Jędrzejewska · Marek Pietrzak ·  
Jerzy Pączkowski

Received: 8 May 2009 / Accepted: 21 July 2009 / Published online: 13 August 2009  
© Springer Science + Business Media, LLC 2009

**Abstract** The study on the relationship between the structure and spectroscopic properties of styrylquinolinium dyes were carried out by measuring the electronic visible absorption, steady-state and time-resolved fluorescence spectra of quinoline based hemicyanine dyes. The influence of the solvent on absorption and emission spectra and the solvatochromic properties, observed for both ground and first excited states, for all the dyes were applied for the evaluation of their excited state dipole moments. The ground state dipole moments of dyes under the study were established by applying *ab initio* calculations. The measured, using solvatochromic methods, excited state dipole moments of tested hemicyanines are in the range from 5.38 to 18.90 D and the change in the dipole moments caused by excitation were found to differ from 1.88 to 6.64 D. It was observed that for all tested dyes the dipole moments of the excited states were higher than those of a ground states. The fluorescence lifetime measurements with picosecond resolution was performed for entire series of hemicyanine dyes possessing different dialkylamino groups attached to the phenyl ring. The average lifetimes of the dye fluorescence, determined from the measured data by multi-order exponential decay curve fitting, were in the range from about 120 to 1200 ps at the fluorescence peak wavelength. The fluorescence lifetime measurements were performed for dyes in ethyl acetate solutions. The time-resolved fluorescence spectra measurements allowed to propose the mechanism of the dyes excited states deactivation.

**Keywords** Styrylquinolinium dyes ·  
Electronic absorption and steady-state fluorescence spectra ·  
Fluorescence lifetimes · Solvatochromic shift ·  
Ground and excited state dipole moments

## Introduction

Intense research activity has been devoted to the synthesis of polymethine cyanine dyes, due to their relative stability, high molar extinction coefficient, high fluorescent intensity etc. They have found a wide application in various fields, such as near-infrared laser dyes and fluorescent labeling agents for proteins. Polymethine cyanine dyes also belong to a well-known class of organic compounds which have been used in photography and information storage, in laser technology and as photopolymerization initiators [1–5].

Dyes, synthesized following a donor- $\pi$ -system-acceptor design concept, play a major role in UV-vis spectrophotometric and/or fluorometric ion analysis [6]. Such compounds usually consist of a macrocyclic or acyclic ion-responsive receptor, often the electron donating moiety, and a heterocyclic or polyaromatic moiety which can function as an electron-deficient acceptor [7]. Furthermore, donor and acceptor can be in direct electronic conjugation *via* an oligomethine  $\pi$ -system ( $-(CH = CH)_n$ ) or a (elongated, for  $n > 1$ ) styrene-type  $\pi$ -system ( $-(CH = CH)_nC_6H_4-$ ). The acceptor moiety itself can (formally) be charged or uncharged [8]. Dyes of the former type are mostly asymmetric hemicyanines and styryls. Those of the latter type are often stilbene-analogue styryl bases. Based on their electronic properties, the spectroscopic behavior of the styryls and styryl bases is often determined by an intramolecular charge transfer (ICT) process accompanying optical excitation.

B. Jędrzejewska (✉) · M. Pietrzak · J. Pączkowski  
Faculty of Chemical Technology and Engineering,  
University of Technology and Life Sciences,  
Seminaryjna 3,  
85-326 Bydgoszcz, Poland  
e-mail: beata@utp.edu.pl

The dipole moment of an electronically excited state of a molecule is an important property that provides information on the electronic and geometrical structure of the molecule in its short-lived state. Among the existing methods for determination of the change in dipole moments associated with electronic excitation of a molecule, the most popular ones are based on a linear correction between the wave-number of the absorption and emission maxima and a solvent polarity function which usually involves both permittivity and the refractive index of the medium [9, 10].

Most theories [11–13, 27] of the solvent effect on the location of the absorption,  $\bar{\nu}_a$ , and fluorescence,  $\bar{\nu}_f$ , bands lead, in spite of different assumptions, to similar expressions for the  $\bar{\nu}_a - \bar{\nu}_f$  and  $\bar{\nu}_a + \bar{\nu}_f$  (see Eqs. 11 and 12) with the difference, however, that the applied solvent polarity parameters  $F(\epsilon, n)$  and  $\phi(\epsilon, n)$  differ significantly.

According to Bilot and Kawski [13] and based on quantum-mechanical second-order perturbation theory for spherical solute molecules centered in a closed spherical microenvironment, the solvent polarity parameters are given by Eqs. (1) and (2):

$$F_{BK}(\epsilon, n) = \frac{\frac{\epsilon-1}{2\epsilon+1} - \frac{n^2-1}{2n^2+1}}{\left(1 - \frac{2\alpha}{a^3} \cdot \frac{\epsilon-1}{2\epsilon+1}\right) \left(1 - \frac{2\alpha}{a^3} \cdot \frac{n^2-1}{2n^2+1}\right)^2} \quad (1)$$

$$g_{BK}(n) = \frac{\frac{n^2-1}{2n^2+1} \left(1 - \frac{\alpha}{a^3} \cdot \frac{n^2-1}{2n^2+1}\right)}{\left(1 - \frac{2\alpha}{a^3} \cdot \frac{n^2-1}{2n^2+1}\right)^2} \quad (2)$$

For an isotropic polarizability of the solute [13], the condition  $2\alpha/a^3=1$  is frequently satisfied, and solvent polarity parameters can be expressed by equations:

$$F_{BK}(\epsilon, n) = \frac{(2n^2 + 1)}{(n^2 + 2)} \cdot \left[ \frac{(\epsilon - 1)}{(\epsilon + 2)} - \frac{(n^2 - 1)}{(n^2 + 2)} \right] \quad (3)$$

$$g_{BK}(n) = \frac{3}{2} \cdot \left[ \frac{(n^4 - 1)}{(n^2 + 2)^2} \right] \quad (4)$$

If the polarizability of the solute is neglected, i.e.  $\alpha=0$ , the equation for  $F(\epsilon, n)$  obtained by Lippert and Mataga et al. [13] results from:

$$F_{LM}(\epsilon, n) = \frac{\epsilon - 1}{2\epsilon + 1} - \frac{n^2 - 1}{2n^2 + 1} \quad (5)$$

According to McRea's theory [13]

$$F_{MR}(\epsilon, n) = \frac{\epsilon - 1}{\epsilon + 2} - \frac{n^2 - 1}{n^2 + 2} \quad (6)$$

In Bakhshiev's theory [13, 14] the functions of the solvent polarity are:

$$F_B(\epsilon, n) = \frac{(2n^2 + 1)}{(n^2 + 2)} \cdot \left[ \frac{(\epsilon - 1)}{(\epsilon + 2)} - \frac{(n^2 - 1)}{(n^2 + 2)} \right] + p^{a-f} \frac{n^2 - 1}{n^2 + 2} \quad (7)$$

$$\phi_B(n) = \frac{2n^2 + 1}{n^2 + 2} \cdot \frac{\epsilon - 1}{\epsilon + 2} + p^s \frac{n^2 - 1}{n^2 + 2} \quad (8)$$

where  $p^{a-f}$  and  $p^s$  are the parameters dependent on the solute properties. These parameters can be determined either by plotting a line through a point for vapours (a free molecule) or, if no data for vapours are available, by preserving the best linearity of the relation examined. By neglecting the second term in (7) we receive (3).

For an ellipsoidal molecule of isotropic polarizability it follows from the general theory of Liptay [11, 13] that the solvent parameters are:

$$F_L(\epsilon, n) = \frac{\epsilon - 1}{\epsilon + 2} - \frac{n^2 - 1}{n^2 + 2} \quad (9)$$

$$\phi_L(\epsilon, n) = \frac{\epsilon - 1}{\epsilon + 2} \quad (10)$$

Equation (9) is identical with (6).

For spherical molecules, in the case of isotropic polarizability of a molecule, based on the theory of Bilot and Kawski [13] and Bakshiev [14], Eqs. (11) and (12) hold:

$$\bar{\nu}_a - \bar{\nu}_f = F_1(\epsilon, n) \frac{2 \cdot (\mu_e - \mu_g)^2}{hca^3} + C_1 \quad (11)$$

$$\bar{\nu}_a + \bar{\nu}_f = -F_2(\epsilon, n) \frac{2 \cdot (\mu_e^2 - \mu_g^2)}{hca^3} + C_2 \quad (12)$$

$\mu_e$  and  $\mu_g$  are the dipole moments in the excited and ground state, respectively,  $h$  is the Planck's constant,  $c$  is the velocity of light in vacuum,  $a$  is Onsager's interaction radius of the solute,  $F_1(\epsilon, n)$  and  $F_2(\epsilon, n)$  are the solvent polarity functions given by Eqs. (3) and (13).

$$F_2(\epsilon, n) = F_1(\epsilon, n) + 3 \cdot \left[ \frac{(n^4 - 1)}{(n^2 + 2)^2} \right] \quad (13)$$

If the ground and excited state dipole moments are parallel, based on Eqs. (11) and (12), Eqs. (14–16) can be derived:

$$\mu_g = \left( \frac{m_2 - m_1}{2} \right) \cdot \left[ \frac{hca^3}{2m_1} \right]^{1/2} \quad (14)$$

$$\mu_e = \left( \frac{m_1 + m_2}{2} \right) \cdot \left[ \frac{hca^3}{2m_1} \right]^{1/2} \quad (15)$$

or

$$\mu_e = \left( \frac{m_1 + m_2}{m_2 - m_1} \right) \cdot \mu_g \quad \text{for } (m_2 > m_1) \quad (16)$$

where  $m_1$  and  $m_2$  are the slopes of the plot obtained using the Eqs. (11) and (12).

Equations (11) and (12) show that for the parallelly orientated dipole moments in the ground and excited states there is no need to estimate Onsager's cavity radius for the calculation of  $\mu_e$ , and  $\mu_g$  as well as that  $\mu_e$  can be calculated directly from the spectroscopic measurements [15].

The present communication deals with study of the spectroscopic behavior of hemicyanine dyes possessing as the electron-deficient moiety quinoline ring. We report the determination of ground and excited state dipole moments by the solvent perturbation method. We also investigate the fluorescence decay lifetimes using time-correlated photon counting technique allowing the fluorescence lifetime with picosecond-time resolution to be measured. The decay lifetimes of the solutions were determined from two- or three-exponential decay fitting.

## Experimental

### Materials

All starting reagents and solvents (spectroscopic grade) were purchased from Aldrich Chemical Co. and used without further purification.

4-[4-(N,N-dialkylamino)-styryl]-1-methyl-quinolinium iodides (marked as series **L**) possessing different amino groups attached to the phenyl ring have been synthesized by the procedures reported in literature [16–20].

### Spectroscopic measurements

Absorption spectra were recorded with a Shimadzu UV-vis Multispec-1501 spectrophotometer, and fluorescence spectra were obtained with a Hitachi F-4500 spectrofluorimeter. Absorption and emission spectra were recorded in a spectroscopic quality: acetonitrile, acetone, 1-methyl-2-

pyrrolidinone (MP), dimethylsulfoxide (DMSO), dimethylformamide (DMF), tetrahydrofuran (THF), ethyl acetate (EtOAc) and 1,4-dioxane. The solvents are characterized by their static dielectric constant ( $\epsilon$ ) at 20°C and refractive index  $n_D$  [21]. The fluorescence measurements were performed at an ambient temperature.

The fluorescence quantum yields of the dyes in ethyl acetate : 1-methyl-2-pyrrolidinone mixture (10:1) were determined as follows. The fluorescence spectrum of a dilute (<25  $\mu$ M) dye solution was recorded by excitation at the absorption band maximum of the standard. A dilute Rodamine B in ethanol ( $\Phi=0.55$  [22]) was used as reference. The fluorescence spectrum of Rodamine B was obtained by excitation at its absorption maximum at 530 nm. The quantum yield of the tested dye ( $\Phi_{\text{dye}}$ ) was calculated using equation:

$$\Phi_{\text{dye}} = \Phi_{\text{ref}} \frac{I_{\text{dye}} A_{\text{ref}}}{I_{\text{ref}} A_{\text{dye}}} \quad (17)$$

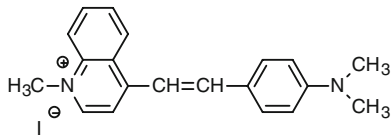
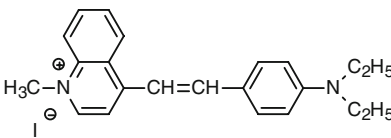
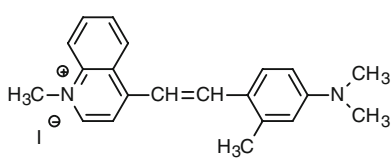
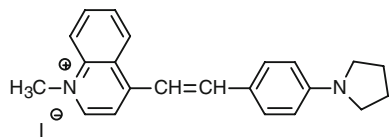
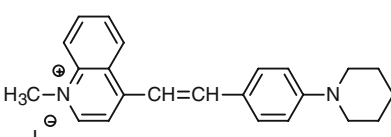
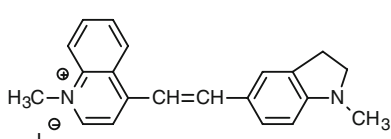
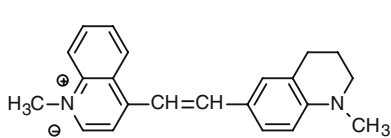
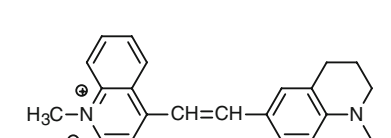
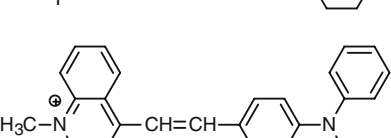
where:  $\Phi_{\text{ref}}$  is the fluorescence quantum yield of reference (Rodamine B) sample in ethanol,  $A_{\text{dye}}$  and  $A_{\text{ref}}$  are the absorbances of the dye and reference samples at the excitation wavelengths (530 nm),  $I_{\text{dye}}$  and  $I_{\text{ref}}$  are the areas arbitrary units of the corrected fluorescence spectra (plotted in frequency scale) for the dyes and reference samples, respectively.

The fluorescence lifetimes were measured using an Edinburgh Instruments, single-photon counting system (FLS920P Spectrometers). The apparatus utilizes for the excitation a picosecond diode laser generating pulses of about 55 ps at 466 nm. Short laser pulses in combination with a fast microchannel plate photodetector and ultrafast electronics make a successful analysis of fluorescence decay signals with a resolution of few picoseconds possible. The dyes were studied at concentration able to provide equivalent absorbance at 466 nm (0.2–0.3 in the 10 mm cell) to be obtained. The fluorescence decays were fitted to two or three exponentials, as necessary. The average lifetime,  $\tau_{\text{av}}$  is calculated as  $\tau_{\text{av}} = (\sum_i \alpha_i \tau_i) / (\sum_i \alpha_i)$ , where  $\alpha_i$  and  $\tau_i$  are the amplitudes and lifetimes. Time-resolved emission spectra (TRES) were calculated from the fit parameters of the multiexponential decays detected from 480 to 840 nm at 10 nm intervals and the corresponding steady-state intensities. The TRES are obtained by spectral reconstruction, which is a relative normalization of the fitted decays to the steady state emission spectrum. Log-normal fitting of TRESs yields emission maxima of TRES.

### Theoretical calculations

The Onsager cavity radii ( $a$ ) of the dye molecules were determined theoretically from molecular models where the

**Table 1** The steady-state spectral properties of styrylquinolinium dyes in acetonitrile and tetrahydrofuran

Dye	Structure	$\lambda_a$	$\lambda_f$	$\Delta\nu$	$\lambda_a$	$\lambda_f$	$\Delta\nu$
		[nm]	[nm]	[cm <sup>-1</sup> ]	[nm]	[nm]	[cm <sup>-1</sup> ]
		tetrahydrofuran			acetonitrile		
L1		542	689	3936	542	697	4103
L2		555	688	3487	555	693	3588
L3		554	691	3579	552	693	3690
L4		560	694	3448	562	703	3569
L5		544	698	4056	550	711	4117
L6		564	710	3646	561	724	4013
L7		568	692	3155	573	719	3548
L8		595	693	2373	597	735	3141
L9		538	689	4074	542	697	4103

molar volumes were calculated. *Ab initio* calculations were carried out using B3LYP/6-311+G (2d,p) method to estimate the ground state dipole moments and the Onsager's cavity radius of the dye molecules under investigation. All calculations were carried out with Gaussian 03 program [23].

#### Dipole moment determination

For the determination of the excited state singlet dipole moments the solvatochromic method, applying the Bakshiev's [14] approach [Eqs. (11) and (12)], was used.

## Results and discussion

### Absorption and fluorescence spectra

The 4-styrylquinolinium dyes L1-L9 of general structure shown in Table 1 possess quinolinium moiety as electron acceptor and different in structure p-N,N-dialkyl(aryl)anilines as electron donating groups. Each dye has a quaternary nitrogen acceptor at one terminus of the chromophoric group and thus assumes a vectorial flow of electron from the substituent in the styryl unit.

The absorption and fluorescence spectra of selected dyes in 1-methyl-2-pyrrolidinone and dimethylsulfoxide are shown in Figs. 1 and 2.

The maxima of absorption and emission spectra positions and the Stokes shifts for styrylquinolinium dyes under the study in two, representative solvents applied are collected in Table 1.

The absorption spectra show a maximum around 550 nm for all the dyes with a shift of the maximum depending on the solvent used. Apart from this, another absorption band around 300 nm is also observed. Only the longest

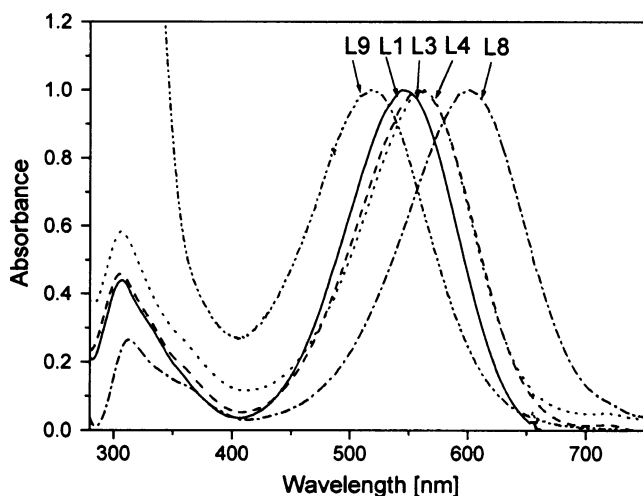


**Fig. 1** Normalized electronic absorption spectra of selected styrylquinolinium dyes in 1-methyl-2-pyrrolidinone (MP)

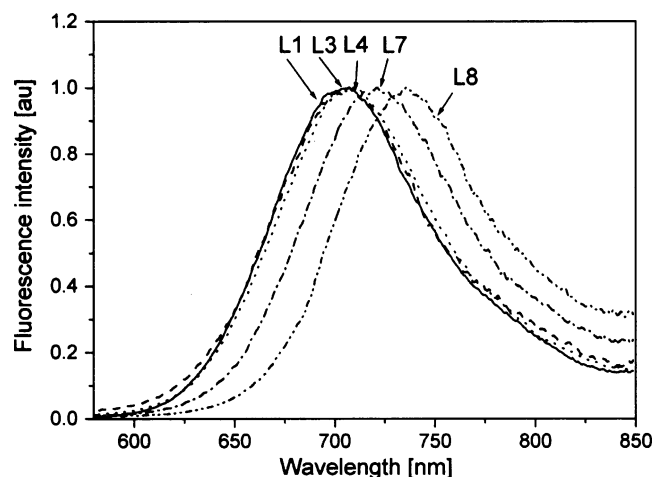


**Fig. 2** Normalized fluorescence spectra of selected styrylquinolinium dyes in dimethylsulfoxide (DMSO)

wavelength band is sensitive to solvent polarity and, therefore, the absorption maximum shift with the solvent is reported only for this band. The emission spectra are recorded by exciting the sample at 530 nm. The excitation maximum coincides with the longest wavelength absorption band that has been assigned as the intramolecular charge transfer transition, due to transfer of charge from the nitrogen in amino group to quinolinium residue. The longest wavelength absorption and emission bands are strongly influenced by the substituent at the 4-position of the phenyl ring. For illustration of this behavior the properties of L1 and L8 dyes are analyzed. In DMF solution both the absorption and emission maxima are shifted from 543 nm and 699 nm to 598 nm and 732 nm, respectively. The bathochromic shift of the spectral maxima with the change of the electron donor substituent is consistent with a charge transfer (CT) character of the

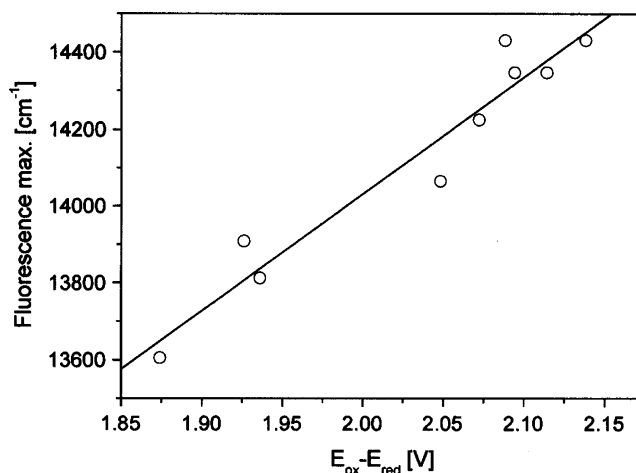


**Fig. 3** Fluorescence frequency of compounds L1-L9 in acetonitrile versus  $E_{ox}(D) - E_{red}(A)$

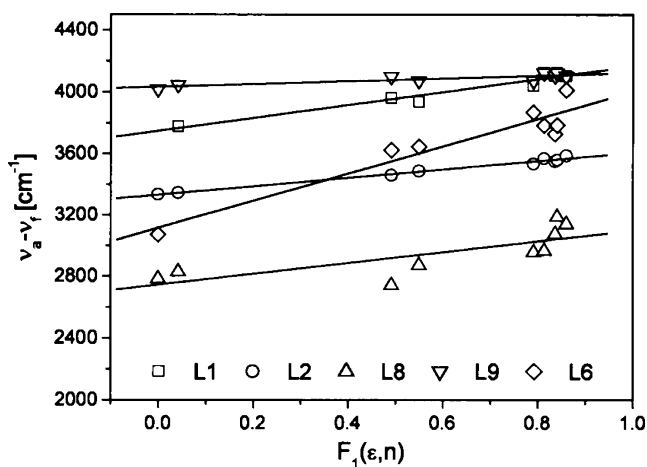


**Fig. 4** Plot  $\nu_a - \nu_f$  [ $\text{cm}^{-1}$ ] vs.  $F_1(\epsilon, n)$  for marked in Figure selected hemicyanine dyes

corresponding electronic transition. These results indicate an electronic interaction between the substituted phenyl ring, as an electron donor, and the quinolinium residue, as an electron acceptor, *via* the styryl double bond. The nice illustrations of this specific interaction are L6-L8 dyes possessing characteristic rigid and planar structure of the amino group in respect to benzene ring causes an increase in delocalization of the lone pair electron at the amino nitrogen to the  $\pi$ -orbital of the dye chromophore cation [24, 25]. In general, the better electron donor is the substituted, the more bathochromically is shifted the CT absorption band.

The absorption and emission spectra of tested dyes were also examined in various solvents characterized by different polarities. In solvents applied for dye with a dimethylamino substituent (L1) the spectral shift of the absorption maxima between the highest and lowest value ( $\Delta\lambda_{\text{max}}$ ), due to change of solvent, is within  $735 \text{ cm}^{-1}$ , whereas dye L8,

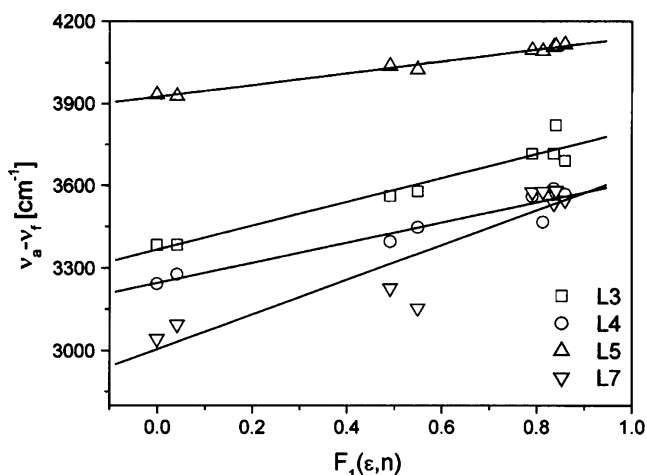


**Fig. 5** Plot  $\nu_a - \nu_f$  [ $\text{cm}^{-1}$ ] vs.  $F_1(\epsilon, n)$  for marked in Figure selected hemicyanine dyes

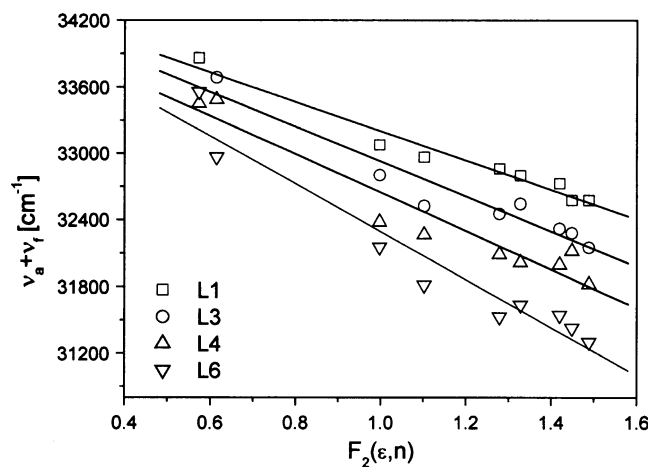


**Fig. 6** Plot  $\nu_a + \nu_f$  [ $\text{cm}^{-1}$ ] vs.  $F_2(\epsilon, n)$  for marked in Figure selected hemicyanine dyes

possessing a stiffened alkylamino group, shows a shift of about  $660 \text{ cm}^{-1}$ . In general, in the absorption spectra the long wavelength absorption band undergoes a hypsochromic shift (absorption peak position blue-shifts) as the solvent polarity increases (negative solvatochromism). This relation allows concluding that the dipole moments of the excited states reached directly after excitation are rather small.

The emission spectra of all the hemicyanines under the study are structureless and have a maximum around  $700 \text{ nm}$ , with the Stokes' shifts depending on the solvent. The emission charge transfer band shows a shift of about  $970 \text{ cm}^{-1}$  in the fluorescence spectra on changing the solvent polarity from low to high. The large bathochromic shifts of the emission bands with increasing the solvent polarity indicate greater stabilization of the excited singlet state in polar solvents. The less pronounced absorption shift with solvent implies that the ground state energy distribution is not affected to a greater extent possibly due to the

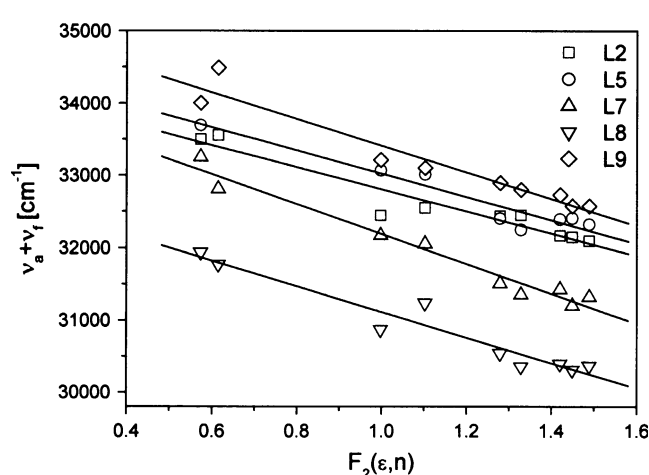


**Fig. 7** Plot  $\nu_a + \nu_f$  [ $\text{cm}^{-1}$ ] vs.  $F_2(\epsilon, n)$  for marked in Figure selected hemicyanine dyes

**Table 2** Slopes of the linear relationship between the spectral shift and the solvent polarity parameters, calculated Onsager's cavity radius, the ground state dipole moments and estimated excited state dipole moments of the tested dyes

Dye denotation	$m_1$	$m_2$	$R^1$	$R^2$	Onsager's radius [Å]	$\mu_g$ [D]	$\mu_e$ [D]	$\mu_e - \mu_g$ [D]	$\mu_e / \mu_g$
L1	418.72	1327.2	0.97	0.98	5.41	2.82	5.38	2.56	1.91
L2	276.61	1528.7	0.99	0.96	5.80	5.22	7.55	2.33	1.45
L3	434.29	1577.7	0.97	0.96	5.66	3.70	6.50	2.80	1.76
L4	366.64	1731	0.96	0.96	5.50	4.74	7.16	2.42	1.51
L5	215.05	1611.4	0.99	0.96	5.52	6.27	8.15	1.88	1.30
L6	888.32	2154.3	0.95	0.97	5.44	2.66	6.46	3.80	2.43
L7	631.17	2061.4	0.93	0.98	5.74	3.89	7.36	3.47	1.89
L8	370.45	1770.7	0.77	0.97	5.73	4.91	7.58	2.67	1.54
L9	1933.5	1583.2	0.87	0.97	6.11	12.26	18.9	6.64	1.54

less polar nature of the dyes in the ground state rather than the excited state. This trend is characteristic for molecules that are likely to have enlarged dipoles and CT characters in their excited singlet states [26].

The structures of acceptor and donor, as Verhoeven et al. [27] documented have strong influence on the energy of the CT state, namely on the CT fluorescence. The energy level of emitting CT state can be described by Eq. 18.

$$E_{CT} = E_{ox}(D) - E_{red}(A) + C \quad (18)$$

where:  $E_{ox}(D)$  and  $E_{red}(A)$  represent the one-electron oxidation and reduction potentials of donor and acceptor and  $C$  is a constant that depends on the degree of charge separation. For the analysis the reduction and oxidation potentials of compounds under the study have been measured by cyclic voltammetry. The correlation between CT fluorescence frequency (in MeCN) and  $E_{ox}(D) - E_{red}(A)$  for L1-L9 is shown in Fig. 3. A linear relationship is observed, documenting that the observed emission occurs from CT state. Similar behavior was earlier observed for other class of hemicyanine dyes studied in our laboratory [18, 28, 29].

#### Determination of the excited state dipole moment

In order to estimate the ground and excited state dipole moments of the molecules, the spectral shifts  $\bar{\nu}_a - \bar{\nu}_f$  and  $\bar{\nu}_a + \bar{\nu}_f$  (in  $\text{cm}^{-1}$ ) for the dyes under the study versus the solvent polarity function  $F_1(\epsilon, n)$  and  $F_2(\epsilon, n)$  were measured. The results of these measurements are shown in Figs. 4, 5, 6 and 7. The linear progression was done and the data were fitted to a straight lines. The slopes  $m_1$  and  $m_2$  of lines shown in Figs. 4, 5, 6 and 7 are listed in the Table 2.

The solvatochromic methods [13, 14, 30–32] applied for determination of the dipole moments of the excited state give for the dyes under the study the linear relationship between the spectral shift and the polarity parameters (dielectric constant and refractive index) of solvents. The correlation coefficients being larger than 0.93 (except the L8 and L9) indicate a good linearity for both  $m_1$  and  $m_2$  factors. All method used gave very similar the excited state dipole moments values (with except of L9 dye), thus indicating colinearity of  $\mu_g$  and  $\mu_e$  vectors.

The dipole moments estimated from the linear relationships and calculated Onsager's cavity radius, evaluated from the

**Table 3** Fluorescence quantum yields, lifetimes, radiative and non-radiative rate constants for hemicyanine dyes under the study

Dye	$\tau_1$ [ps]	$A_1$	$\tau_2$ [ps]	$A_2$	$\tau_3$ [ps]	$A_3$	$\tau_{av}$ [ps]	$\phi_f$	$k_f/10^7$ [ $\text{s}^{-1}$ ]	$k_{nr}/10^9$ [ $\text{s}^{-1}$ ]
L1	63.87	86.82	263.58	3.23	1209.98	9.95	120.76	0.0118	9.77	8.18
L2	108.05	74.71	365.06	18.78	2013.61	6.52	482.68	0.0125	2.59	2.05
L3	47.86	59.05	534.63	20.08	2417.78	20.88	625.38	0.0074	1.19	1.59
L4	91.87	65.75	437.29	26.63	1811.6	7.62	576.16	0.0133	2.31	1.71
L5	85.99	11.11	360.5	65.12	1722.64	23.78	1217.06	0.0130	1.07	0.81
L6	46.78	45.15	377.37	16.51	1695.81	38.34	445.78	0.0034	0.76	2.24
L7	58.57	60.4	339.24	21.13	1403.34	18.47	394.56	0.0060	1.53	2.52
L8	122.25	34.28	284.23	22.26	1228.73	43.46	639.18	0.0088	1.38	1.55
L9	100.23	84.95	263.41	8.26	1532.75	6.79	229.64	0.0033	1.44	4.34

molecules optimized geometries, for styrylquinolinium dyes under the study are summarized in Table 2.

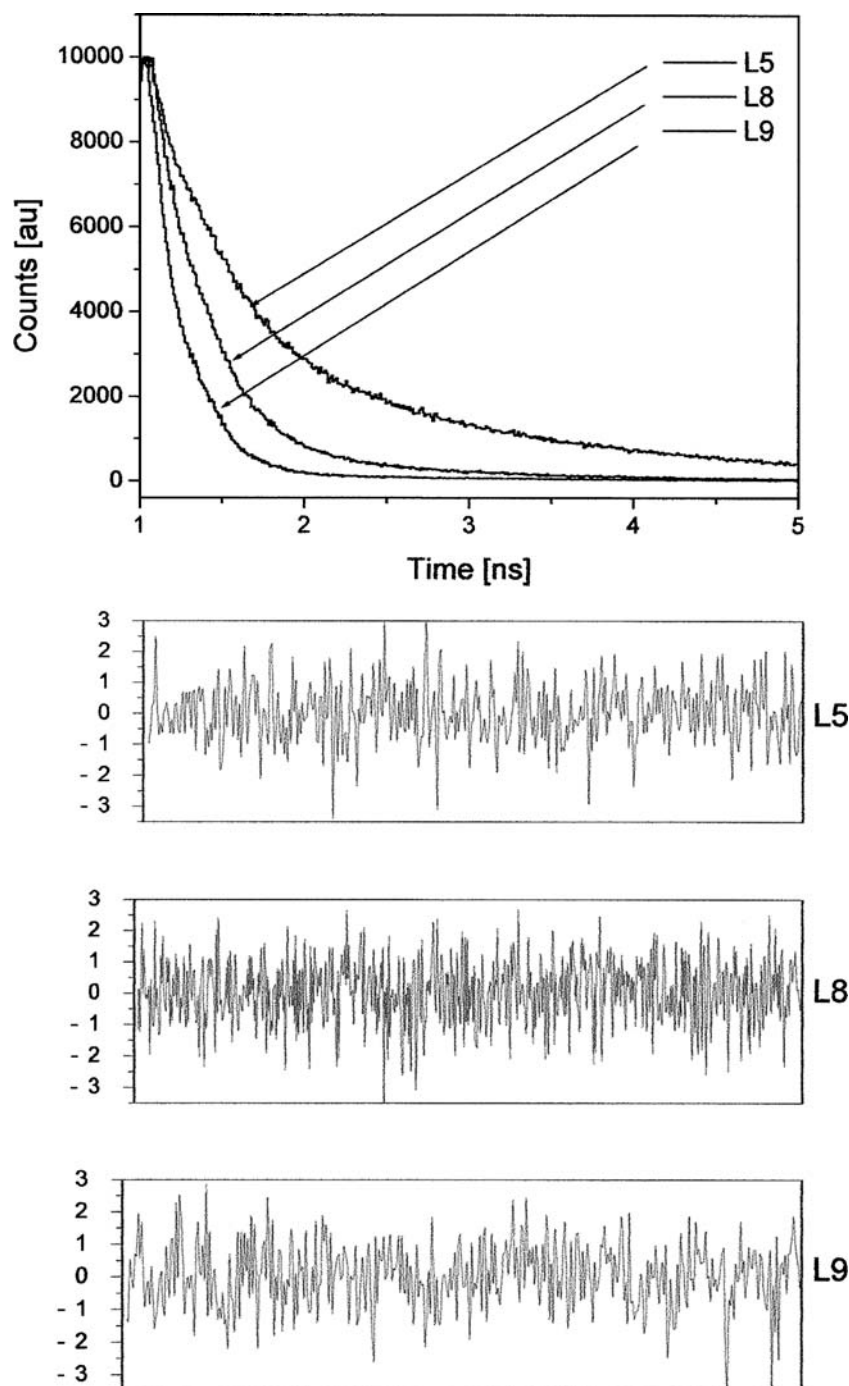
The calculated values of the cavity radius for **L1-L9** dyes are in the range of 5.41–6.11 Å. This value is rather small compared to the molecular length of the dyes which are about 15–16 Å.

The obtained results show that the excited state dipole moments of hemicyanine dyes under the study in their excited state are in the range from 5.38 to 18.90 D and are higher than those calculated for the ground state. The

evaluated differences ( $\mu_e - \mu_g$ ) oscillates between 1.88 D and 6.64 D. The changes in the dipole moments on the electronic excitation ( $\mu_e - \mu_g$ ) depend on the dye structure. The calculated changes in the dipole moments upon excitation corresponds to an intermolecular displacement of a charge upon excitation oscillating in the range from 0.39 to 1.38 Å.

Inspection of the data presented in Table 2 reveal that for all dye molecules under investigation, the changes in the dipole moments on the electronic excitation are rather

**Fig. 8** The fluorescence decay curves of selected hemicyanines (L5, L8, L9) recorded in ethyl acetate - 1-methyl-2-pyrrolidone (10:1) solution;  $\lambda_{EX} = 466$  nm;  $\lambda_{EM} = 650$  nm





small. This suggests that the emission of these dyes originate from states, which although are more polar than the ground state, are probably similar to the locally excited states (FC excited state).

#### Fluorescence quantum yield and lifetime

The most common method to determine the absolute quantum yield of fluorescence involves comparison with a standard material emitting with a known efficiency. We chose Rhodamine B dissolved in ethanol ( $A=0.1$  at 530 nm) as a reference substance. The fluorescence quantum efficiency of this dye is well established and equals 0.55 [22].

The fluorescence efficiency of the styrylquinolinium dyes are compiled in Table 3. The values are rather small and are dependent on the structure of a dialkylamino group substituted in the phenyl ring. The fluorescence quantum yield decreases with increasing of the electron-donating ability of the amino substituent. The low fluorescence quantum yields, characteristic for styrylquinolinium dyes possessing electron donating substituents in phenyl ring, can be attributed, at least in part, to the photoinduced intramolecular charge transfer (ICT) interaction, which contributes effectively to fluorescence quenching.

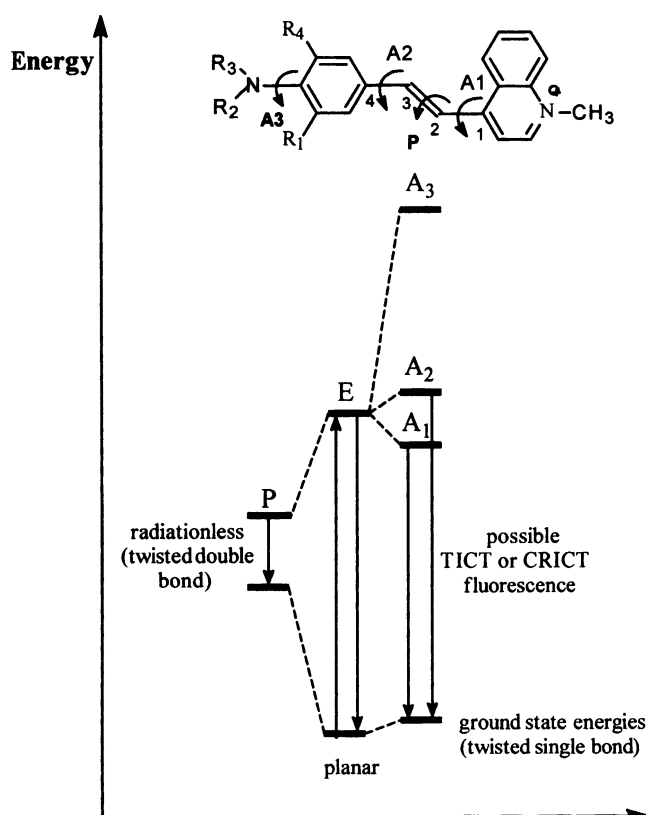
Figure 8 shows the fluorescence decay curves of selected hemicyanine dyes in ethyl acetate. In order to extract the quantitative values of the decay lifetimes from the experimental fluorescence curves, the three-exponential decay functions were used for nonlinear curve fitting. From the three-exponential decay functions, the fast decay lifetime for L1 is fitted to the value of about 64 ps ( $\tau_1$ ), the middle to 264 ps ( $\tau_2$ ) and the slow one to 1210 ps ( $\tau_3$ ), yielding averaged time ( $\tau_{av}$ ) equals  $\tau_{av} = (A_1\tau_1 + A_2\tau_2 + A_3\tau_3)/(A_1 + A_2 + A_3) = 120.7$ ps.

The decay lifetimes of the hemicyanine dyes solution from previous reports ranges from 17 ps [14] to 200 ps [33]. The observed difference can be due to the changes in the polarity of the solvent or to the hemicyanine derivative used, and finally to the limited time resolution of the Time-Correlated Single Photon Counting (TCSPC) methods applied [33–35].

As can be seen in Fig. 8, the fluorescent behaviors of the dyes seem to present an appreciable change caused by the amino alkyl substituents in phenyl ring. The fitting results for the different dyes are summarized in Table 3. The fluorescence lifetime lack of similarity difference is considered to not be within the experimental uncertainties and suggests that the amino alkyl substituent influence the possible rotation about the dye double bond.

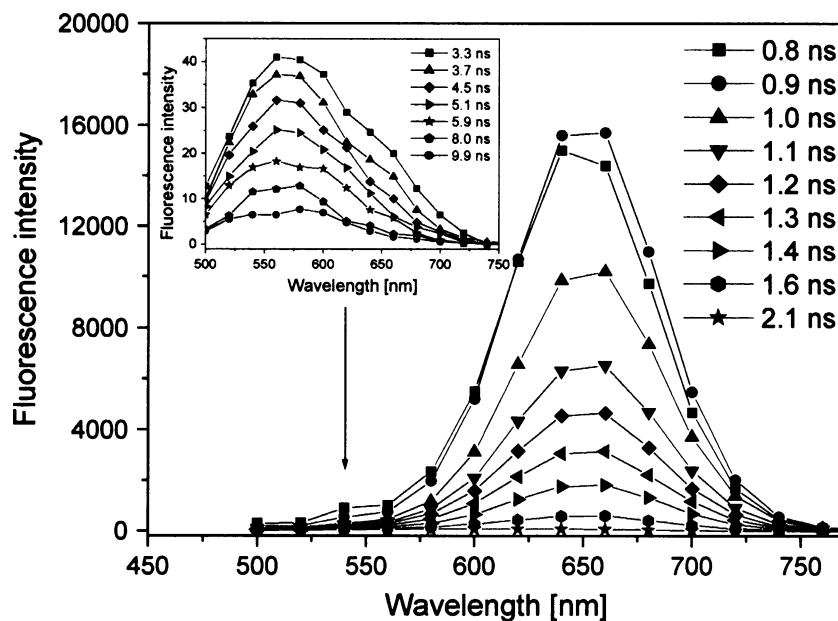
The molecules under investigation can be treated as D- $\pi$ -A salts. In literature there are two different explanations that describe observed photophysical behaviour of salts of this type. The first adopts the model developed for stilbene

photoisomerization that assumed the presence of so-called “phantom state” being, according to Hammond et al. [36] twisted stilbene triplet state. In the “phantom state” the dye exists in a quinoid form with a  $90^\circ$  twist of the two aromatic planes on either side of the double bond. This perpendicular configuration (labeled as  $Q_\perp$ ) can exist in other dyes with similar structures such as hemicyanines and dyes used in this study. This model was successfully adopted by Ikeda et al. [37] for the description of amino-styrylpyridinium dyes photophysics. The  $Q_\perp$  form in hemicyanine dyes may be stabilized by the intramolecular charge transfer (ICT) from pyridinium to dialkyl amino group [34]. In more polar solvents the benzenoid form dominates due to hydrogen bonding between solvents and dimethylamino group, whereas the quinoid form is stabilized in nonpolar solvent. Since the “phantom state” can be the triplet state in nature, its lifetime should be longer than that for molecule singlet state. Thus, according to this model, the longest luminescence lifetime recorded for D- $\pi$ -A salts can be attributed to the emission from the perpendicular quinoid ( $Q_\perp$ ) or ICT state (the “phantom state”). The fluorescence shortest time observed ( $\tau_1 < 0.08$  ns) can be attributed to the emission from trans isomer, and finally the middle lifetime ( $\tau = 0.1$ – $0.7$  ns) is due to the emission from cis form.



**Scheme 1** Conceptual presentation of the different conformations of hemicyanine dyes as predicted by Rettig et al. [33]

**Fig. 9** Time-resolved emission spectra of L1 in ethyl acetate – 1-methyl-2-pyrrolidinone (10:1) solution recorded at room temperature;  $\lambda_{EX}=466$  nm



The second explanation of specific photophysical properties of stilbazolium salts is given by Rettig et al. [38]. These authors applied the global analysis technique to construct the spectral profile of several emitting states. A global fit of the emission data, obtained from time-resolved fluorescence spectroscopy, for the molecules tested by Rettigs group, showed that a multi-exponential model was necessary in order to obtain acceptable fit.

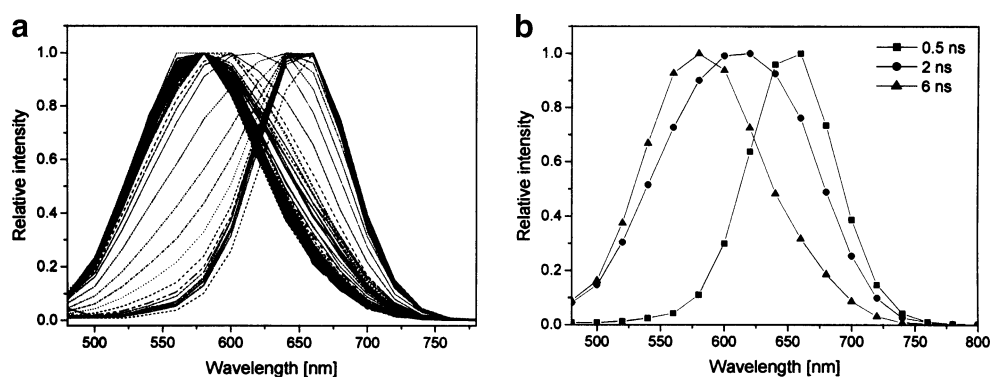
According to the Rettig model [38] simultaneous fluorescence can occur from the initially reached excited state with planar conformation (E) and the two twisting states ( $A_1$  and  $A_2$ ) formed as a results of a rotation around both of the single bonds of the olefinic styryl group (see Scheme 1). These twistings lead to two twisted intramolecular charge transfer (TICT) states with an energy close to that of relaxed Franck-Condon state. The twist of the dialkylamino group leads to a TICT state, however its energy level is considerably higher than for non-twisted conformation, therefore it can not be easily thermally activated and to contribute in the emission spectra. A twist of the double bond gives a state with a relatively narrow  $S_1$ -

$S_0$  gap. The deactivation of this state should be radiationless in character because of a small energy gap to the ground state. A simultaneous fluorescence from E,  $A_1$  and/or  $A_2$  is therefore a likely explanation for the broad steady state spectra measured and for the multiple fluorescence decay.

The excited-state decay kinetics we represent as a series of time-resolved emission spectra (TRES) corresponding to particular instants of time. To reconstruct TRES for L1 in ethyl acetate—1-methyl-2-pyrrolidinone (10:1) solution, the corresponding emission decays recorded at a series of wavelengths spanning the steady state emission spectrum have been recorded. Log-normal fitting of TRESs yields two emission maxima (Fig. 9).

Characteristic two emissive bonds are observed upon transition from the initial red to the final blue spectra. The main fluorescence spectrum occurring at shorter times shows a maximum around 660 nm whereas for longer times the fluorescence reaches a maximum of about 560 nm. The analysis of the fluorescence lifetime distributions at different emission wavelengths indicates that two major emissive excited-states are present (Fig. 10).

**Fig. 10** Area-normalized time-resolved emission spectra of L1 in ethyl acetate – 1-methyl-2-pyrrolidinone (10:1) solution at room temperature at different time delays after excitation; A: The spectra shift to shorter wavelengths. The first spectrum on the right corresponds to time zero, and each subsequent spectrum corresponds to a shift of 0.1 ns. The last presented spectrum is at 10 ns



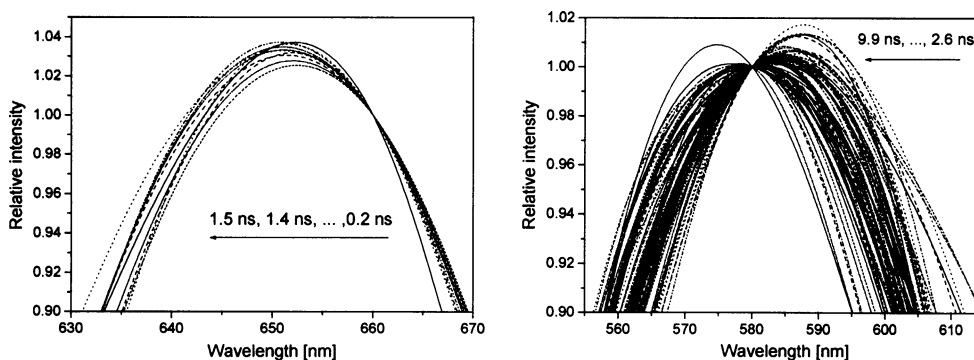


**Fig. 11** Area-normalized time-resolved emission spectra of L1 in ethyl acetate – 1-methyl-2-pyrrolidinone (10:1) solution at both longer and shorter wavelength region measured at different time delays after excitation (time delay changed every 0.1 ns from right to left)

The measured and the evaluated photophysical properties for dyes under the study, e.g. fluorescence quantum yields ( $\phi_f$ ), lifetime ( $\tau_f$ ), radiative ( $k_r$ ) and non-radiative ( $k_{nr}$ ) rate constants are presented in Table 3. The rate constants of the radiative and nonradiative processes of the excited singlet state were calculated according to the relations [39]:

$$k_r = \frac{\phi_f}{\tau_f} \quad (19)$$

$$k_{nr} = \frac{(1 - \phi_f)}{\tau_f} \quad (20)$$

The data compiled in Table 3 show that for tested dyes the non-radiative transition rates are two order of magnitude faster than the radiative rates. The non-radiative rate includes contribution of the excited singlet state to the photoisomerization reaction, the singlet-triplet intersystem crossing and the internal conversion processes.

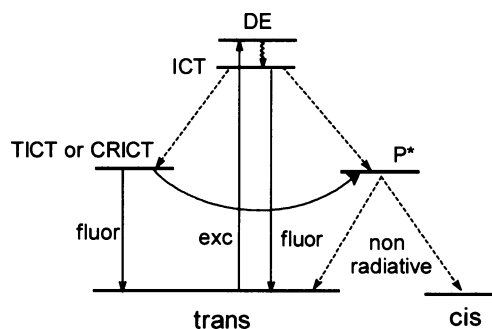
The spectroscopic and lifetime results indicate the existence of emitting multiple species of the styrylquinolinium dye. The multiple fluorescence can in principle be due to:

- i) a possible transition of  $\pi \rightarrow \pi^*$  locally excited state (LE) to the charge-transfer (CT) state
- ii) the intramolecular relaxation of the  $\pi \rightarrow \pi^*$  locally excited state involving  $A_1$  and  $A_2$  rotations (see Scheme 1).

Figure 11 shows the presence of characteristic two emissive points at both longer and shorter wavelength regions. The presence of a characteristic iso-emissive point at about 660 and 580 nm supports the prediction that two major interconverting excited states populations are present for both emissions.

The interpretation of multiple fluorescence of tested hemicyanine dyes, considering obtained results can be based on the three-state kinetic scheme (Scheme 2) proposed by Rettig et al. [38] and then modified by Abraham et al. [40].

According to the Scheme 2 after excitation of the nearly planar molecule the excited state is directly formed. This excited state may be assign to an intramolecular charge transfer state (ICT) formed during a time shorter than the pulse duration ( $< 1$  ps) after vertical transition of the so-called delocalized excited DE state [41]. From this state isomerization can occur by population of the  $P^*$  state with non-radiative transition. The  $P^*$  state is less polar than the ICT state. Increasing solvent polarity stabilizes the ICT state (lower energy minimum) without changing the  $P^*$  state configuration. Thus, the energy barrier  $ICT \rightarrow P^*$  increases with solvent polarity. Alternatively the twisting of one or both single bonds neighboring the olefinic double bond according to the TICT mechanism lead to an intermediate state (TICT or CRICT). The TICT excited state is formed when the twist is complete and goes to  $90^\circ$ . Whereas, the conformational relaxed ICT (CRICT) state is formed from the ICT state by barrierless relaxation through single bond twisting when some twisting angle exists which increases the dipole moment and the polarity of this state more than the ICT state. The formation rate of this CRICT state is controlled by the solvent viscosity and polarity which dramatically changes the barrier crossing owing to the dipole moment of the CRICT state. Since the relaxation channel from ICT to CRICT state is very fast compared to



**Scheme 2** Model for the interpretation of the photophysical behavior of donor-acceptor compounds [35]

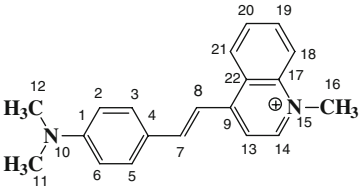
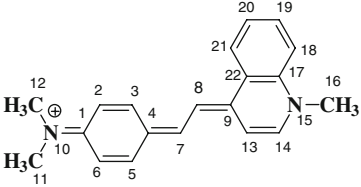
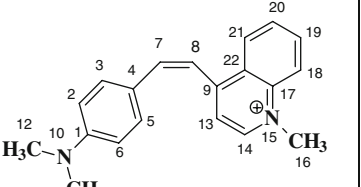
the relaxation channel between ICT and P\* state, the route for isomerization is practically hindered in polar solvents [38, 40–42].

The structural mobility of planar dye molecules has been suggested to be a possible cause of the internal conversion, depending on the  $\pi$ -electron density in the electronic excited

state. Table 4 summarized the quantum chemical calculations of the electron density for geometric and conformational isomers of the simplest styrylquinolinium dye L1.

From the theoretical calculations it was deduced that the major changes in net atomic charges occur only on few atoms of the dye in the vicinity of the styryl bond.

**Table 4** The enthalpy of molecule formation and the electron density calculated for geometric and conformational isomers of the simplest styrylquinolinium dye

No	Electron density		
			
1	0.676	0.651	0.723
2	-0.226	-0.201	-0.213
3	-0.445	-0.455	-0.040
4	0.523	0.558	1.011
5	-0.225	-0.215	-0.658
6	-0.221	-0.177	-0.283
7	0.078	-0.005	-0.438
8	0.052	0.139	-0.442
9	0.989	0.937	1.280
10	-0.068	-0.029	-0.062
11	0.129	0.159	0.129
12	0.145	0.176	0.146
13	-0.462	-0.458	-0.774
14	0.080	0.042	0.377
15	0.098	0.095	0.095
16	0.185	0.176	0.203
17	0.081	0.080	0.192
18	-0.382	-0.395	-0.348
19	-0.146	-0.176	-0.177
20	-0.277	-0.285	-0.278
21	-0.079	-0.109	-0.282
22	0.493	0.489	0.831

Therefore, it is reasonable to expect that this part of molecule plays a dominant role in the solvation dynamics because of the changes in atomic charges. The *ab initio* calculations indicate that the bond length of the central C4-C7, C7-C8 and C8-C9 bonds show single-double-single bonds characters with values equals to 1.427, 1.377 and 1.426 Å for trans and 1.436, 1.378 and 1.435 Å for cis forms, respectively, confirming the ethenic linkage character in the ground state. The values of bond angles C4-C7-C8 and C7-C8-C9 are equal 127.61 and 125.5 for trans and 133.62 and 131.17 for cis forms, respectively. The torsion angle of twisting of electron donor and electron acceptor parts of molecule around bridging moiety (C4-C7-C8-C9 atoms) are equal 180.0 and 19.0 for trans and cis form, respectively, which suggests a planar structure for trans form in the ground state.

The enthalpy of the quinoid form formation  $\Delta H_f$  is higher than that calculated for ground state, by about 146.5 kJ mol<sup>-1</sup> which indicates that the trans conformation of L1 dominates in the ground state while the quinoid structure is more favorable in the excited.

The importance of a stable perpendicular quinoid ( $Q_{\perp}$ ) configuration in the ground state of asymmetric dyes such as cyanine dyes has been discussed in literature particularly in a nonpolar medium [43, 44]. The quinoid form was proposed to be quasi-stable in the ground state [43] but experimental results were supportive of stable quinoid form in excited state only [43].

The foregoing results indicate clearly that combination of a substituted phenyl ring with a quinoline moiety through an ethylenic bridge provides a unique family of tunable intrinsic fluorophores. For such a family, changes in the electronic polarization (due to introduction of different substitution groups), solvation and rotation free volumes are translated into changes in their spectral behavior and the fluorescence characteristics. Highly emissive tunable chromophores are rare [45] although they have been attracting considerable interest as compounds for fluorescent sensors and switches [46].

## Conclusions

The spectroscopic behavior of the hemicyanine dyes in solvents of different polarity has been compared. It was observed that the shifts of emission peaks with change in solvent polarity are more pronounced than the shifts of absorption peaks, indicating that  $\mu_e \gg \mu_g$ , i.e. the dipole moments of the molecules increase on excitation. We also reported the results of the measurements of the fluorescence quantum efficiency of nine styrylquinolinium dyes relatively to Rhodamine B in ethanol and the fluorescence lifetimes. The results revealed three-exponential decay of the emission spectra in ethyl acetate.

**Acknowledgment** This work was supported by The Ministry of Science and Higher Education (MNiSW) (grants No NN204 054135 and NN204 054335).

## References

- Robert G, Dawid W, Jon B, Paul R (1996) The isomerisation of meso-amine substituted heptamethine dyes. *Dyes Pigm* 30:321–332
- El-Aal RMA (2004) Thiazoline and thiazoloxazole in synthesis of novel meso-substituted mono-tri-, and hepta-methine cyanine dyes. *Dyes Pigm* 61:251–261
- James TH (1977) The theory of the photographic process, 4th edn. Macmillan, New York
- Moeda M (1984) Laser dyes. Academic, Tokyo
- Chatterjee S, Gottschalk P, Davis PD, Schuster GB (1988) Electron-transfer reactions in cyanine borate ion pairs: photopolymerization initiators sensitive to visible light. *J Am Chem Soc* 110:2326–2328
- Rettig W, Lapouyade R (1994) In: Lakowicz JR (ed) Probe design and chemical sensing. Plenum, New York, p 109
- Valeur B (1994) In: Lakowicz JR (ed) Probe design and chemical sensing. Plenum, New York, p 21
- Bricks JL, Slominskii JL, Kudinova MA, Tolmachev AI, Rurack K, Resch-Genger U, Rettig W (2000) Syntheses and photophysical properties of a series of cation-sensitive polymethine and styryl dyes. *J Photochem Photobiol A: Chem* 132:193–208
- Inamdar SR, Nadaf YF, Mulimani BG (2003) Ground and excited state dipole moments of exalite 404 and exalite 417 UV laser dyes determined from solvatochromic shifts of absorption and fluorescence spectra. *J Molec Struct (Theochem)* 624:47–51
- Ghazy R, Azim SA, Shaheen M, El-Mekawey F (2004) Experimental studies on the determination of the dipole moments of some different laser dyes. *Spectrochim. Acta Part A* 60:187–191
- Liptay W (1974) In: Lim EC (ed) Excited States, vol. 1. Academic, INC New York, pp 129–229
- Baumann W (1989) In Rossiter BW, Hamilton JF (Eds) Physical Methods of Chemistry, vol. 38. John Wiley and Sons, pp 45–131
- Kawski A (2002) On the estimation of excited state dipole moments from solvatochromic shifts of absorption and fluorescence spectra. *Z Naturforsch* 57a:255–262
- Bakshiev NG (1964) *Opt Spectrosc (USSR)* 16:821–832.
- Kawski A (1992) In: Rabek JF (ed) Progress in photochemistry and photophysics 5, (Chapter 1). CRC, Boca Raton, USA, pp 1–47
- Heterocyclic polymethine dyes. Synthesis, properties and application (2008) In Strekowski L (Ed) Topic in heterocyclic chemistry, vol. 14, Springer-Verlag Berlin Heidelberg
- Mishra A, Behera RK, Behera PK, Mishra BK, Behera GB (2000) Cyanines during the 1990s: a review. *Chem Rev* 100:1973–2011
- Wróblewski S, Trzebiatowska K, Jędrzejewska B, Pietrzak M, Gawinecki R, Pączkowski J (1999) Developing of fluorescence probes based on stilbazonium salts for monitoring free radical polymerization processes. *J Chem Soc Perkin Trans 2*:1909–1917
- Zhou Y-f, Feng S-y, Wang X-m, Zhao X, Jiang M-h (2002) Study on two-photon properties of a new series of chromophores. *J Molec Struct* 609(1–3):67–71
- Bahner CT, Pace ES, Prevost R (1951) Quaternary salts of styryl pyridines and quinolines. *J Am Chem Soc* 73(7):3407–3408
- Reichardt Ch (1988) Solvent and solvent effects in organic chemistry. VCH Publishers, Weinheim, Germany, pp 365–371

22. Ozçelik S (2002) Steady state and picosecond time-resolved photophysics of a benzimidazolocarbocyanine dye. *J Luminesc* 96:141–148
23. Gaussian 03, Revision B.03, Frisch MJ, Trucks GW, Schlegel HB, Scuseria GE, Robb MA, Cheeseman JR, Montgomery JA Jr, Vreven T, Kudin KN, Burant JC, Millam JM, Iyengar SS, Tomasi J, Barone V, Mennucci B, Cossi M, Scalmani G, Rega N, Petersson GA, Nakatsuji H, Hada M, Ehara M, Toyota K, Fukuda R, Hasegawa J, Ishida M, Nakajima T, Honda Y, Kitao O, Nakai H, Klene M, Li X, Knox JE, Hratchian HP, Cross JB, Adamo C, Jaramillo J, Gomperts R, Stratmann RE, Yazyev O, Austin AJ, Cammi R, Pomelli C, Ochterski JW, Ayala PY, Morokuma K, Voth GA, Salvador P, Dannenberg JJ, Zakrzewski VG, Dapprich S, Daniels AD, Strain MC, Farkas O, Malick DK, Rabuck AD, Raghavachari K, Foresman JB, Ortiz JV, Cui Q, Baboul AG, Clifford S, Cioslowski J, Stefanov BB, Liu G, Liashenko A, Piskorz P, Komaromi I, Martin RL, Fox DJ, Keith T, Al-Laham MA, Peng CY, Nanayakkara A, Challacombe M, Gill PMW, Johnson B, Chen W, Wong MW, Gonzalez C, Pople JA, Gaussian, Inc., Pittsburgh PA, 2003
24. Lang AD, Huang CH, Gan LB, Zhou DJ (1999) Studies of the photocurrent generation performances from a series of amphiphilic bis-chromophore zinc complexes and correlation between photocurrent generation performance and molecular structure. *Syn Met* 99:97–103
25. Fayed TA, El-Din S, Etaiw H, Khatib HM (2005) Excited state properties and acid–base equilibria of *trans*-2-styrylbenzoxazoles. *J Photochem Photobiol A: Chem* 170:97–103
26. Bosch P, Fernandez-Arizpe A, Mateo JL, Lozano AE, Noheda P (2000) New fluorescent probes for monitoring polymerisation reactions: 1. Synthesis, solvatochromism and emission properties. *J Photochem Photobiol A: Chem* 133:51–57
27. Hermant RM, Bakker NAC, Scerer T, Krijnen B, Verhoeven JW (1999) Systematic study of a series of highly fluorescent rod-shaped donor-acceptor systems. *J Am Chem Soc* 112:1214–1221
28. Kabatc J, Jędrzejewska B, Bajorek A, Pączkowski J (2006) Stilbene-like molecules as fluorescent probes applied for monitoring of polymerization process. *J Fluoresc* 16(4):525–534
29. Jędrzejewska B, Jeziórska J, Pączkowski J (2008) Studies on an argon laser induced photopolymerization employing both mono- and bischromophoric hemicyanine dye–borate complex as a photoinitiator. *J Photochem Photobiol A* 195:105–115
30. Suppan P (1990) Invited review solvatochromic shifts: The influence of the medium on the energy of electronic states. *J Photochem Photobiol A Chem* 50:293–330
31. Fayed TA (1999) Intramolecular charge transfer and photoisomerization of 2-(*p*-dimethylaminostyryl)benzoxazole: A new fluorescent probe. *J Photochem Photobiol A Chem* 121:17–25
32. Raikar US, Renuka CG, Nadaf YF, Mulimani BG, Karguppikar AM (2006) Rotational Diffusion and Solvatochromic Correlation of Coumarin 6 Laser Dye. *J. Fluoresc* 16:847–854
33. Kim J, Lee M, Yang J-H, Choy J-H (2000) Photophysical Properties of Hemicyanine Dyes Intercalated in Na–Fluorine Mica. *J Phys Chem A* 104:1388–1392
34. Mishra A, Behera GB, Kriszna MMG, Periasamy N (2001) Time-resolved fluorescence studies of aminostyryl pyridinium dyes in organic solvents and surfactant solutions. *J. Luminescence* 92:175–188
35. Kim J, Lee M (1999) Excited-state photophysics and dynamics of a hemicyanine dye in AOT reverse micelles. *J Phys Chem A* 103:3378–3382
36. Hammond GS, Saltiel J, Lamola AA, Turro NS, Breadshaw JS, Cowan DO, Consuell RC, Vogt V, Dalton C (1964) Mechanisms of photochemical reactions in solution. XXII. <sup>1</sup> Photochemical *cis-trans* isomerization. *J Am Chem Soc* 86:3197–3217
37. Ikeda N, Mataga N, Steiner U, Abdel-Kader MH (1983) Picosecond laser photolysis studies upon photochemical isomerization and protolytic reaction of a stilbazolium betaine. *Chem Phys Lett* 95:66–71
38. Strehmel B, Seifert H, Rettig W (1997) Photophysical properties of fluorescence probes. 2. A model of multiple fluorescence for stilbazolium dyes studied by global analysis and quantum chemical calculations. *J Phys Chem B* 101(12):2232–2243
39. Kosower EM, Giniger R, Radkowsky A, Hebel D, Shustennan A (1986) Bimanes 22. Flexible fluorescent molecules. Solvent effects on the photophysical properties of syn-bimanes (1, 5-diazabicyclo[3.3.0]octa-3, 6-diene-2, 8-diones). *J Phys Chem* 90:5552–5557
40. Abraham E, Oberlé J, Jonusauskas G, Lapouyade R, Rullière C (1997) Dual excited states in 4-dimethylamino 4'-cyanostilbene (DCS) revealed by sub-picosecond transient absorption and Kerr ellipsometry. *J. Photochem Photobiol A Chem* 105:101–107
41. Locke RJ, Lim EC (1987) Intermolecular interactions between pairs of electronically excited molecules; evidence for “bicimer” formation in 1, 1-di- $\alpha$ -naphthylmethane. *Chem Phys Lett* 134: 107–109
42. Lapouyade R, Czeschka K, Majenz W, Rettig W, Gilbert E, Rullière C (1992) Photophysics of donor-acceptor substituted stilbenes. A time-resolved fluorescence study using selectively bridged dimethylamino cyano model compounds. *J Phys Chem* 96:9643–9650
43. Ponterini G, Monicchioli F (1991) Trans-cis photoisomerization mechanism of carbocyanines: experimental check of theoretical models. *Chem Phys* 151:111–126
44. Dietz F, Rentsch SK (1985) On the mechanism of photoisomerization and the structure of the photoisomers of cyanine dyes. *Chem Phys* 96:145–151
45. Joshi HS, Jamshidi R, Tor Y (1999) Conjugated 1, 10-phenanthrolines as tunable fluorophores. *Angew Chem Int* 38:2722–2725
46. Czarnik AW (1992) Fluorescent chemosensors for ion and molecule recognition. American Chemical Society, Washington